

Multimodal Chain-of-Thought Reasoning in Language Models

Zhuosheng Zhang¹ Aston Zhang² Mu Li² Hai Zhao¹ George Karypis² Alex Smola²

Abstract

Large language models (LLMs) have shown impressive performance on complex reasoning by leveraging chain-of-thought (CoT) prompting to generate intermediate reasoning chains as the rationale to infer the answer. However, existing CoT studies have focused on the language modality. We propose Multimodal-CoT that incorporates language (text) and vision (images) modalities into a two-stage framework that separates rationale generation and answer inference. In this way, answer inference can leverage better generated rationales that are based on multimodal information. With Multimodal-CoT, our model under 1 billion parameters outperforms the previous state-of-the-art LLM (GPT-3.5) by 16% (75.17%→91.68%) on the ScienceQA benchmark and even surpasses human performance. Code is publicly available.¹

1. Introduction

Imagine reading a textbook with no figures or tables. Our ability to knowledge acquisition is greatly strengthened by jointly modeling diverse data modalities, such as vision, language, and audio. Recently, large language models (LLMs) (Brown et al., 2020; Thoppilan et al., 2022; Rae et al., 2021; Chowdhery et al., 2022) have shown impressive performance in complex reasoning by generating intermediate reasoning steps before inferring the answer. The intriguing technique is called chain-of-thought (CoT) reasoning (Wei et al., 2022b; Kojima et al., 2022; Zhang et al., 2022).

However, existing studies related to CoT reasoning are largely isolated in the language modality (Wang et al., 2022b; Zhou et al., 2022; Lu et al., 2022b; Fu et al., 2022), with little consideration of multimodal scenarios. To elicit CoT reasoning in multimodality, we advocate a Multimodal-CoT paradigm. Given the inputs in different modalities,

¹Shanghai Jiao Tong University ²Amazon Web Services. Correspondence to: Zhuosheng Zhang (work done at Amazon Web Services) <zhangzs@sjtu.edu.cn>, Aston Zhang <astonz@amazon.com>.

¹<https://github.com/amazon-science/mm-cot>

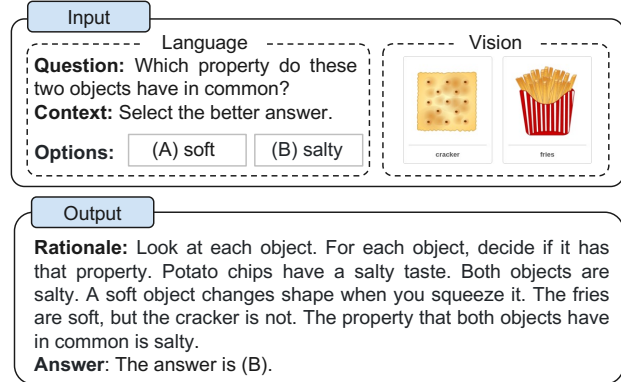


Figure 1. Example of the multimodal CoT task.

Multimodal-CoT decomposes multi-step problems into intermediate reasoning steps (rationale) and then infers the answer. Since vision and language are the most popular modalities, we focus on those two modalities in this work. An example is shown in Figure 1. In general, there are two ways to elicit Multimodal-CoT reasoning as follows: (i) prompting LLMs and (ii) fine-tuning small models.²

The most immediate way to perform Multimodal-CoT is to transform the input of different modalities into one modality and prompt LLMs to perform CoT. For example, it is possible to extract the caption of an image by a captioning model and then concatenate the caption with the original language input to be fed into LLMs (Lu et al., 2022a). However, there is severe information loss in the captioning process; thus, using the captions (as opposed to vision features) may suffer from a lack of mutual synergy in the representation space of different modalities.

To facilitate the interaction between modalities, another potential solution is to fine-tune smaller language models (LMs) by fusing multimodal features (Zhang et al., 2023). As this approach allows the flexibility of adjusting model architectures to incorporate multimodal features, we study fine-tuning models in this work instead of prompting LLMs. The key challenge is that language models under 100 billion parameters tend to generate hallucinated rationales that mislead the answer inference (Ho et al., 2022; Magister et al., 2022; Ji et al., 2022).

²In this work, we refer to small models as models with less than 1 billion parameters (hereinafter dubbed as 1B-models).

Table 1. Typical CoT techniques (FT: fine-tuning; KD: knowledge distillation). Segment 1: in-context learning techniques; Segment 2: fine-tuning techniques. To the best of our knowledge, our work is the first to study CoT reasoning in different modalities. Besides, we focus on 1B-models, without relying on the outputs of LLMs.

Models	Mutimodal	w/o LLM	Model / Engine	Training	CoT Role	CoT Source
Zero-Shot-CoT (Kojima et al., 2022)	✗	✗	GPT-3.5 (175B)	ICL	Reasoning	Template
Few-Shot-CoT (Wei et al., 2022b)	✗	✗	PaLM (540B)	ICL	Reasoning	Hand-crafted
Self-Consistency-CoT (Wang et al., 2022a)	✗	✗	Codex (175B)	ICL	Reasoning	Hand-crafted
Least-to-Most Prompting (Zhou et al., 2022)	✗	✗	Codex (175B)	ICL	Reasoning	Hand-crafted
Retrieval-CoT (Zhang et al., 2022)	✗	✗	GPT-3.5 (175B)	ICL	Reasoning	Auto-generated
PromptPG-CoT (Lu et al., 2022b)	✗	✗	GPT-3.5 (175B)	ICL	Reasoning	Hand-crafted
Auto-CoT (Zhang et al., 2022)	✗	✗	Codex (175B)	ICL	Reasoning	Auto-generated
Complexity-CoT (Fu et al., 2022)	✗	✗	GPT-3.5 (175B)	ICL	Reasoning	Hand-crafted
Few-Shot-PoT (Chen et al., 2022)	✗	✗	GPT-3.5 (175B)	ICL	Reasoning	Hand-crafted
UnifiedQA (Lu et al., 2022a)	✗	✓	T5 (770M)	FT	Explanation	Crawled
Fine-Tuned T5 XXL (Magister et al., 2022)	✗	✗	T5 (11B)	KD	Reasoning	LLM-generated
Fine-Tune-CoT (Ho et al., 2022)	✗	✗	GPT-3 (6.7B)	KD	Reasoning	LLM-generated
Multimodal-CoT (our work)	✓	✓	T5 (770M)	FT	Reasoning	Crawled

To mitigate the challenge of hallucination, we propose Multimodal-CoT that incorporates language (text) and vision (images) modalities into a two-stage framework that separates rationale generation and answer inference. In this way, answer inference can leverage better generated rationales that are based on multimodal information. Our experiments are conducted on the ScienceQA benchmark (Lu et al., 2022a), which is the latest multimodal reasoning benchmark with annotated reasoning chains. Experimental results show that our method surpasses the previous state-of-the-art GPT-3.5 model by +16% (75.17%→91.68%) on the benchmark. Our contributions are summarized as follows:

- (i) To the best of our knowledge, this work is the first to study CoT reasoning in different modalities.
- (ii) We propose a two-stage framework by fine-tuning language models to fuse vision and language representations to perform Multimodal-CoT. The model is able to generate informative rationales to facilitate inferring final answers.
- (iii) Our method achieves new state-of-the-art performance on the ScienceQA benchmark, outperforming accuracy of GPT-3.5 by 16% and even surpassing human performance.

2. Background

This section reviews recent progress of eliciting CoT reasoning by prompting and fine-tuning language models.

2.1. CoT Reasoning with LLMs

Recently, CoT has been widely used to elicit the multi-step reasoning abilities of LLMs (Wei et al., 2022b). Concretely, CoT techniques encourage the LLM to generate intermediate reasoning chains for solving a problem. Studies have shown that LLMs can perform CoT reasoning with two major paradigms of techniques: Zero-Shot-CoT (Kojima et al., 2022) and Few-Shot-CoT (Wei et al., 2022b; Zhang et al.,

2022). For Zero-Shot-CoT, Kojima et al. (2022) showed that LLMs are decent zero-shot reasoners by adding a prompt like “Let’s think step by step” after the test question to invoke CoT reasoning. For Few-Shot-CoT, a few step-by-step reasoning demonstrations are used as conditions for inference. Each demonstration has a question and a reasoning chain that leads to the final answer. The demonstrations are commonly obtained by hand-crafting or automatic generation. The corresponding techniques are thus referred to as Manual-CoT (Wei et al., 2022b) and Auto-CoT (Zhang et al., 2022).

With effective demonstrations, Few-Shot-CoT often achieves stronger performance than Zero-Shot-CoT and has attracted more research interest. Therefore, most recent studies focused on how to improve Few-Shot-CoT. Those studies are categorized into two major research lines: (i) optimizing the demonstrations; (ii) optimizing the reasoning chains. Table 1 compares typical CoT techniques.

Optimizing Demonstrations The performance of Few-Shot-CoT relies on the quality of demonstrations. As reported in Wei et al. (2022b), using demonstrations written by different annotators results in dramatic accuracy disparity in a symbolic reasoning task. Beyond hand-crafting the demonstrations, recent studies have investigated ways to optimize the demonstration selection process. Notably, Rubin et al. (2022) retrieved the semantically similar demonstrations with the test instance. However, this approach shows a degraded performance when there are mistakes in the reasoning chains (Zhang et al., 2022). To address the limitation, Zhang et al. (2022) found that the key is the diversity of demonstration questions and proposed Auto-CoT: (i) partition questions of a given dataset into a few clusters; (ii) sample a representative question from each cluster and generate its reasoning chain using Zero-Shot-CoT with simple heuristics. In addition, reinforcement learning (RL) and complexity-based selection strategies were also proposed

to obtain effective demonstrations. [Fu et al. \(2022\)](#) chose examples with complex reasoning chains (i.e., with more reasoning steps) as the demonstrations. [Lu et al. \(2022b\)](#) trained an agent to find optimal in-context examples from a candidate pool and maximize the prediction rewards on given training examples when interacting with GPT-3.5.

Optimizing Reasoning Chains A notable way to optimize reasoning chains is problem decomposition. [Zhou et al. \(2022\)](#) proposed least-to-most prompting to decompose complex problems into sub-problems and then solve these sub-problems sequentially. As a result, solving a given sub-problem is facilitated by the answers to previously solved sub-problems. Similarly, [Khot et al. \(2022\)](#) used diverse decomposition structures and designed different prompts to answer each sub-question. In addition to prompting the reasoning chains as natural language texts, [Chen et al. \(2022\)](#) proposed program-of-thoughts (PoT), which modeled the reasoning process as a program and prompted LLMs to derive the answer by executing the generated programs. Another trend is to vote over multiple reasoning paths for a test question. [Wang et al. \(2022a\)](#) introduced a self-consistency decoding strategy to sample multiple outputs of LLMs and then took a majority over the final answers. [Wang et al. \(2022b\)](#) and [Li et al. \(2022b\)](#) introduced randomness in the input space to produce more diverse outputs for voting.

2.2. Eliciting CoT Reasoning by Fine-Tuning Models

A recent interest is eliciting CoT reasoning by fine-tuning language models. [Lu et al. \(2022a\)](#) fine-tuned the encoder-decoder T5 model on a large-scale dataset with CoT annotations. However, a dramatic performance decline is observed when using CoT to infer the answer, i.e., generating the reasoning chain before the answer (reasoning). Instead, CoT is only used as an explanation after the answer. [Magister et al. \(2022\)](#) and [Ho et al. \(2022\)](#) employed knowledge distillation by fine-tuning a student model on the chain-of-thought outputs generated by a larger teacher model. The proposed methods showed performance gains in arithmetic, commonsense, and symbolic reasoning tasks.

There is a key challenge in training 1B-models to be CoT reasoners. As observed by [Wei et al. \(2022b\)](#), models under 100 billion parameters tend to produce illogical CoT that leads to wrong answers. In other words, it might be harder for 1B-models to generate effective CoT than directly generating the answer. It becomes even more challenging in a multimodal setting where answering the question also requires understanding the multimodal inputs. In the following part, we will explore the challenge of Multimodal-CoT and investigate how to perform effective multi-step reasoning.

3. Challenge of Multimodal-CoT

Existing studies have suggested that the CoT reasoning ability may emerge in language models at a certain scale, e.g., over 100 billion parameters ([Wei et al., 2022a](#)). However, it remains an unresolved challenge to elicit such reasoning abilities in 1B-models, let alone in the multimodal scenario. This work focuses on 1B-models as they can be fine-tuned and deployed with consumer-grade GPUs (e.g., 32G memory). In this section, we will investigate why 1B-models fail at CoT reasoning and study how to design an effective approach to overcome the challenge.

3.1. Towards the Role of CoT

To begin with, we fine-tune a text-only baseline for CoT reasoning on the ScienceQA benchmark ([Lu et al., 2022a](#)). Following [Lu et al. \(2022a\)](#), we adopt UnifiedQA_{Base} ([Khashabi et al., 2020](#)) as the backbone language model.³ Our task is modeled as a text generation problem, where the model takes the textual information as the input and generates the output sequence that consists of the rationale and the answer. As an example shown in Figure 1, the model takes the concatenation of tokens of the question text (Q), the context text (C), and multiple options (M) as the input. To study the effect of CoT, we compare the performance with three variants: (i) No-CoT which predicts the answer directly (QCM→A); (ii) Reasoning where answer inference is conditioned to the rationale (QCM→RA); (iii) Explanation where the rationale is used for explaining the answer inference (QCM→AR).

Table 2. Effects of CoT in the one-stage setting.

Method	Format	Accuracy
No-CoT	QCM→A	80.40
Reasoning	QCM→RA	67.86
Explanation	QCM→AR	69.77

Surprisingly, we observe a ↓12.54% accuracy decrease (80.40%→67.86%) if the model predicts rationales before answers (QCM→RA). The results imply that the rationales might not necessarily contribute to predicting the right answer. A similar phenomenon was observed in [Lu et al. \(2022a\)](#), where the plausible reason might be that the model exceeds the maximum token limits before obtaining the required answer or stops generating the prediction early. However, we find that the maximum length of the generated outputs (RA) is always less than 400 tokens, which is below the length limit of language models (i.e., 512 in UnifiedQA_{Base}). Therefore, it deserves a more in-depth investigation into why the rationales harm answer inference.

³UnifiedQA ([Khashabi et al., 2020](#)) is adopted as it is the best fine-tuning model in [Lu et al. \(2022a\)](#). Model information and implementation details are presented in Appendix B.1.

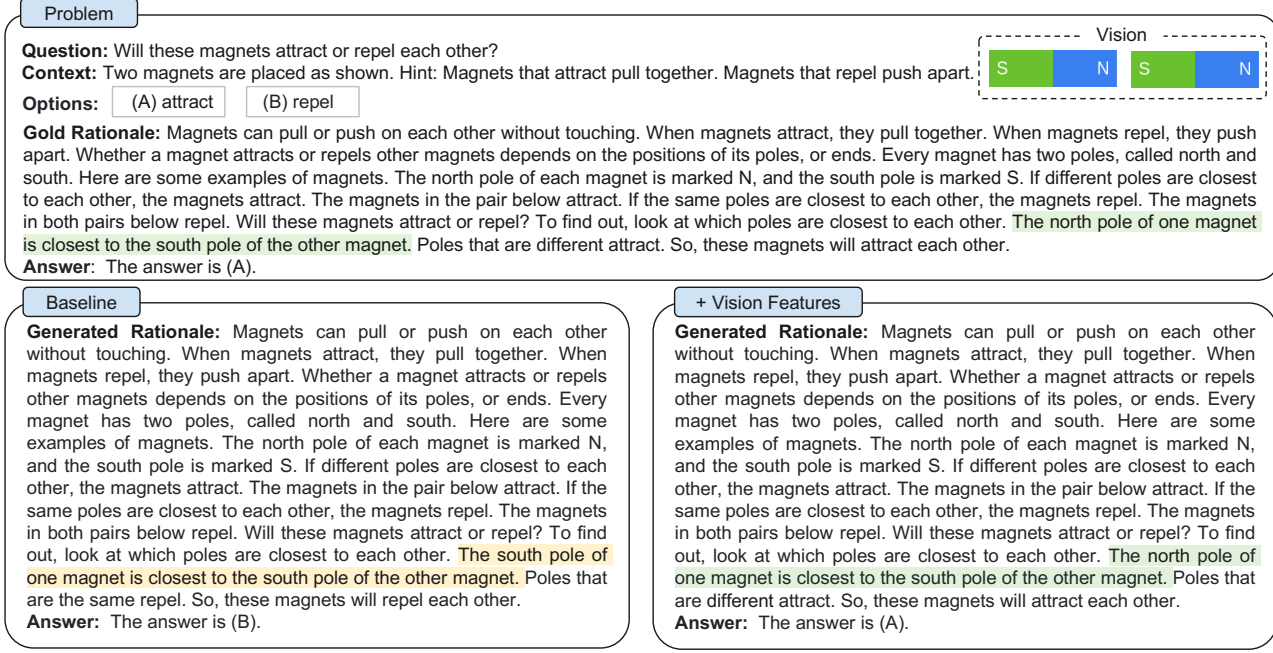


Figure 2. Example of the two-stage framework without vision features (baseline) and with vision features (ours) for generating rationales and predicting answers. The upper part presents the problem details with a gold rationale, and the lower part shows the outputs of the baseline and our method incorporated with vision features. We observe that the baseline fails to predict the right answer due to the misleading by hallucinated rationales. More examples are shown in Appendix A.1.

3.2. Misleading by Hallucinated Rationales

To dive into how the rationales affect the answer prediction, we separate the CoT problem into two stages, *rationale generation* and *answer inference*. We report the RougeL score and accuracy for the rationale generation and answer inference, respectively. Table 3 shows the results based on the two-stage framework. Although the two-stage baseline model achieves a 91.76 RougeL score of the rationale generation, the answer inference accuracy is only 70.53%. Compared with the QCM \rightarrow A variant (80.40%) in Table 2, the result shows that the generated rationale in the two-stage framework does not improve answer accuracy.

Table 3. Two-stage setting of (i) rationale generation (RougeL) and (ii) answer inference (Accuracy).

Method	(i) QCM \rightarrow R	(ii) QCMR \rightarrow A
Two-Stage Framework	91.76	70.53
w/ Captions	91.85	71.12
w/ Vision Features	96.97	84.91

Then, we randomly sample 50 error cases and find that the model tends to generate hallucinated rationales that mislead the answer inference. As an example shown in Figure 2, the model (left part) hallucinates that, “*The south pole of one magnet is closest to the south pole of the other magnet*”, due to the lack of reference to the vision content. We find that such mistakes occur at a ratio of 64% among the error cases

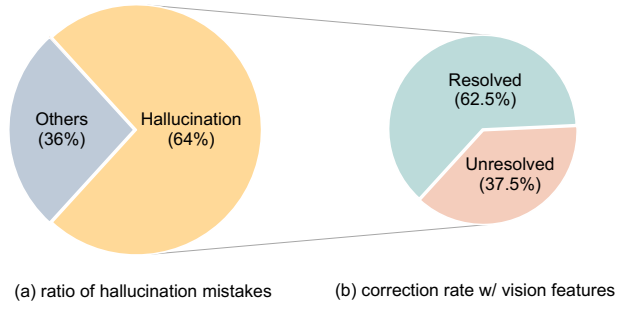


Figure 3. The ratio of hallucination mistakes (a) and correction rate w/ vision features (b).

(Figure 3(a)).

3.3. Multimodality Contributes to Effective Rationales

We speculate that such a phenomenon of hallucination is due to a lack of necessary vision contexts for performing effective Multimodal-CoT. To inject vision information, a simple way is to transform the paired image into a caption (Lu et al., 2022a) and then append the caption in the input of both stages. However, as shown in Table 3, using captions only yields marginal performance gains ($\uparrow 0.59\%$). Then, we explore an advanced technique by incorporating vision features into the language model. Concretely, we feed the paired image to the DETR model (Carion et al., 2020) to extract vision features. Then we fuse the vision features

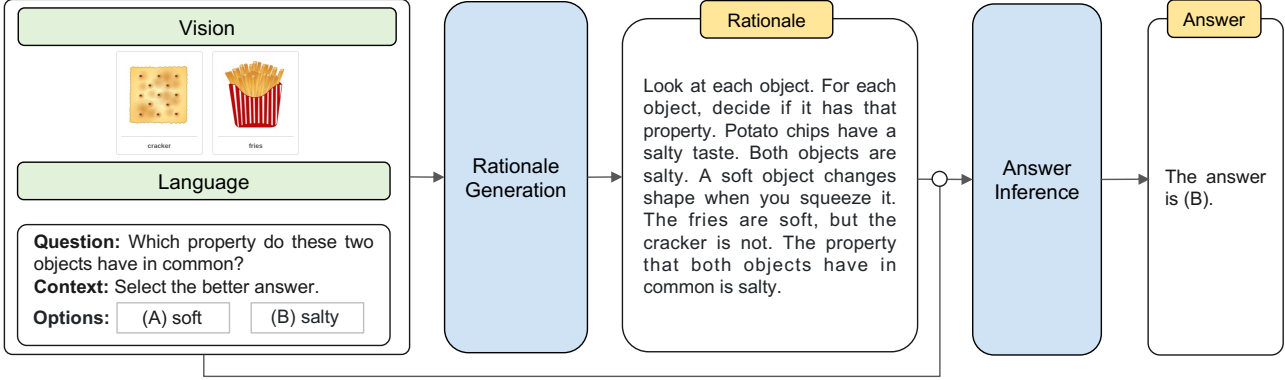


Figure 4. Overview of our Multimodal-CoT framework. Multimodal-CoT consists of two stages: (i) rationale generation and (ii) answer inference. Both stages share the same model architecture but differ in the input and output. In the first stage, we feed the model with language and vision inputs to generate rationales. In the second stage, we append the original language input with the rationale generated from the first stage. Then, we feed the updated language input with the original vision input to the model to infer the answer.

with the encoded language representations before feeding to the decoder (more details will be presented in Section 4). Interestingly, with vision features, the RougeL score of the rationale generation has boosted to 96.97% (QCM \rightarrow R), which correspondingly contributes to better answer accuracy of 84.91% (QCMR \rightarrow A). With those effective rationales, the phenomenon of hallucination is mitigated — 62.5% hallucination mistakes in Section 3.2 have been corrected (Figure 3(b)), as an example shown in Figure 2 (right part).⁴ The analysis so far compellingly shows that vision features are indeed beneficial for generating effective rationales and contributing to accurate answer inference. As the two-stage method (QCMR \rightarrow A) in Table 3 achieves better performance than all the one-stage method in Table 2, we choose the two-stage method in our Multimodal-CoT framework.

4. Multimodal-CoT

Based on the observations and discussions in Section 3, we propose Multimodal-CoT to incorporate language (text) and vision (images) modalities into a two-stage framework. In this section, we will first overview the procedure of the framework and then elaborate on the technical design of the model architecture.

4.1. Framework Overview

Multimodal-CoT consists of two training stages: (i) rationale generation and (ii) answer inference. Both stages share the same model architecture but differ in the input X and output Y . The overall procedure is illustrated in Figure 4. We will take vision-language as an example to show how Multimodal-CoT works.

⁴The left mistakes are mainly about map understanding, which requires more advanced vision features. We will discuss them in Section 6.4.

In the rationale generation stage, we feed the model with $X = \{X_{\text{language}}^1, X_{\text{vision}}\}$ where X_{language}^1 represents the language input in the first stage and X_{vision} represents the vision input, i.e., the image. For example, X can be instantiated as a concatenation of question, context, and options of a multiple choice reasoning problem (Lu et al., 2022a) as shown in Figure 4. The goal is to learn a rationale generation model $R = F(X)$ where R is the rationale.

In the answer inference stage, the rationale R is appended to the original language input X_{language}^1 to construct the language input in the second stage, $X_{\text{language}}^2 = X_{\text{language}}^1 \circ R$ where \circ denotes concatenation. Then, we feed the updated input $X' = \{X_{\text{language}}^2, X_{\text{vision}}\}$ to the answer inference model to infer the final answer $A = F(X')$.

In both stages, we train two models with the same architecture independently. They take the annotated elements (e.g., $X \rightarrow R$, $XR \rightarrow A$, respectively) from the training set for supervised learning. During inference, given X , the rationales for the test sets are generated using the model trained in the first stage; they are used in the second stage for answer inference.

4.2. Model Architecture

Given the language input $X_{\text{language}} \in \{X_{\text{language}}^1, X_{\text{language}}^2\}$ and the vision input X_{vision} , we compute the probability of generating target text Y (either the rationale or the answer in Figure 4) of length N by

$$p(Y|X_{\text{language}}, X_{\text{vision}}) = \prod_{i=1}^N p_{\theta}(Y_i | X_{\text{language}}, X_{\text{vision}}, Y_{<i}), \quad (1)$$

where $p_{\theta}(Y_i | X_{\text{language}}, X_{\text{vision}}, Y_{<i})$ is implemented with a Transformer-based network (Vaswani et al., 2017). The network has three major procedures: encoding, interaction,

Algorithm 1 Multimodal-CoT

Input: Language input X_{language}^1 , vision input X_{vision}
Output: Generated rationale R , inferred answer A

- 1: Construct the input $X = \{X_{\text{language}}, X_{\text{vision}}\}$
- 2: Generate rationale $R = F(X)$ using the model $F(\cdot)$
- 3: Append the rationale R to the original language input $X_{\text{language}}^2 = X_{\text{language}}^1 \circ R$.
- 4: Construct new input $X' = \{X_{\text{language}}^2, X_{\text{vision}}\}$
- 5: Infer the answer A by conditioning on the new input, $A = F(X')$.
- 6: **procedure** $F(X)$
- 7: Encode the language and vision inputs H_{language} and H_{vision} , respectively
- 8: Build the interaction between language and vision features by attention $H_{\text{vision}}^{\text{attn}}$
- 9: Fuse H_{language} and $H_{\text{vision}}^{\text{attn}}$ by a gated fusion mechanism to have H_{fuse}
- 10: Feed H_{fuse} to the decoder to obtain the target prediction Y
- 11: **return** Y
- 12: **end procedure**

and decoding. Specifically, we feed the language text into a Transformer encoder to obtain a textual representation, which is then interacted and fused with the vision representation before being fed into the Transformer decoder.

Encoding The model $F(X)$ takes both the language and vision inputs and obtains the text representation H_{language} and the image feature H_{vision} by the following functions:

$$H_{\text{language}} = \text{LanguageEncoder}(X_{\text{language}}), \quad (2)$$

$$H_{\text{vision}} = W_h \cdot \text{VisionExtractor}(X_{\text{vision}}), \quad (3)$$

where $\text{LanguageEncoder}(\cdot)$ is implemented as a Transformer model. We use the hidden states of the last layer in the Transformer encoder as the language representation $H_{\text{language}} \in \mathbb{R}^{n \times d}$ where n denotes the length of the language input, and d is the hidden dimension. Meanwhile, $\text{VisionExtractor}(\cdot)$ is used to vectorize the input image into vision features. Inspired by the recent success of Vision Transformers (Dosovitskiy et al., 2021), we fetch the patch-level features by off-the-shelf vision extraction models,⁵ such as DETR (Carion et al., 2020). After obtaining the patch-level vision features, we apply a learnable projection matrix W_h to convert the shape of $\text{VisionExtractor}(X_{\text{vision}})$ into that of H_{language} ; thus we have $H_{\text{vision}} \in \mathbb{R}^{m \times d}$ where m is the number of patches.

Interaction After obtaining language and vision representations, we use a single-head attention network to correlate text tokens with image patches, where the query (\mathcal{Q}), key (\mathcal{K}) and value (\mathcal{V}) are H_{language} , H_{vision} and H_{vision} , respec-

⁵The parameters of the vision extraction are frozen.

tively. The attention output $H_{\text{vision}}^{\text{attn}} \in \mathbb{R}^{n \times d}$ is defined as:

$$H_{\text{vision}}^{\text{attn}} = \text{Softmax}\left(\frac{\mathcal{Q}\mathcal{K}^{\top}}{\sqrt{d_k}}\right)\mathcal{V}, \quad (4)$$

where d_k is the same as the dimension of H_{language} because a single head is used.

Then, we apply the gated fusion mechanism (Zhang et al., 2020; Wu et al., 2021; Li et al., 2022a) to fuse H_{language} and H_{vision} . The fused output $H_{\text{fuse}} \in \mathbb{R}^{n \times d}$ is obtained by:

$$\lambda = \text{Sigmoid}(W_l H_{\text{language}} + W_v H_{\text{vision}}^{\text{attn}}), \quad (5)$$

$$H_{\text{fuse}} = (1 - \lambda) \cdot H_{\text{language}} + \lambda \cdot H_{\text{vision}}^{\text{attn}}, \quad (6)$$

where W_l and W_v are learnable parameters.

Decoding Finally, the fused output H_{fuse} is fed into the Transformer decoder to predict the target Y . The complete procedure of Multimodal-CoT is shown in Algorithm 1.

5. Experiments

This section will present the benchmark dataset, the implementation of our technique, and the baselines for comparisons. Then, we will report our main results and findings.

5.1. Dataset

Our method is evaluated on the ScienceQA benchmark (Lu et al., 2022a). ScienceQA is the first large-scale multimodal science question dataset that annotates the answers with detailed lectures and explanations. It contains 21k multimodal multiple choice questions with rich domain diversity across 3 subjects, 26 topics, 127 categories, and 379 skills. The benchmark dataset is split into training, validation, and test splits with 12726, 4241, and 4241 examples, respectively.

5.2. Implementation

The following part presents the experimental settings of Multimodal-CoT and the baseline methods.

Experimental Settings As the Multimodal-CoT task requires generating the reasoning chains and leveraging the vision features, we use the T5 encoder-decoder architecture (Raffel et al., 2020). Specifically, we adopt UnifiedQA (Khashabi et al., 2020) to initialize our models in the two stages because it achieves the best fine-tuning results in Lu et al. (2022a). To verify the generality of our approach across different LMs, we also employ FLAN-T5 (Chung et al., 2022) as the backbone in Section 6.3. As using image captions does not yield significant performance gains in Section 3.3, we did not use the captions. We fine-tune the models up to 20 epochs, with a learning rate of 5e-5. The

Table 4. Main results (%). Size = backbone model size. Question classes: NAT = natural science, SOC = social science, LAN = language science, TXT = text context, IMG = image context, NO = no context, G1-6 = grades 1-6, G7-12 = grades 7-12. Results except ours are taken from Lu et al. (2022a). Segment 1: Human performance; Segment 2: VQA baselines; Segment 3: UnifiedQA baselines; Segment 4: GPT-3.5 baselines; Segment 5: Our Multimodal-CoT results. Results in **bold** are the best performance.

Model	Size	NAT	SOC	LAN	TXT	IMG	NO	G1-6	G7-12	Avg
Human	-	90.23	84.97	87.48	89.60	87.50	88.10	91.59	82.42	88.40
MCAN (Yu et al., 2019)	95M	56.08	46.23	58.09	59.43	51.17	55.40	51.65	59.72	54.54
Top-Down (Anderson et al., 2018)	70M	59.50	54.33	61.82	62.90	54.88	59.79	57.27	62.16	59.02
BAN (Kim et al., 2018)	112M	60.88	46.57	66.64	62.61	52.60	65.51	56.83	63.94	59.37
DFAF (Gao et al., 2019)	74M	64.03	48.82	63.55	65.88	54.49	64.11	57.12	67.17	60.72
ViLT (Kim et al., 2021)	113M	60.48	63.89	60.27	63.20	61.38	57.00	60.72	61.90	61.14
Patch-TRM (Lu et al., 2021)	90M	65.19	46.79	65.55	66.96	55.28	64.95	58.04	67.50	61.42
VisualBERT (Li et al., 2019)	111M	59.33	69.18	61.18	62.71	62.17	58.54	62.96	59.92	61.87
UnifiedQA _{Base} (Khashabi et al., 2020)	223M	68.16	69.18	74.91	63.78	61.38	77.84	72.98	65.00	70.12
UnifiedQA _{Base} w/ CoT (Lu et al., 2022a)	223M	71.00	76.04	78.91	66.42	66.53	81.81	77.06	68.82	74.11
GPT-3.5 (Chen et al., 2020)	175B	74.64	69.74	76.00	74.44	67.28	77.42	76.80	68.89	73.97
GPT-3.5 w/ CoT (Lu et al., 2022a)	175B	75.44	70.87	78.09	74.68	67.43	79.93	78.23	69.68	75.17
Mutimodal-CoT _{Base}	223M	87.52	77.17	85.82	87.88	82.90	86.83	84.65	85.37	84.91
Mutimodal-CoT _{Large}	738M	95.91	82.00	90.82	95.26	88.80	92.89	92.44	90.31	91.68

Table 5. Ablation results of Multimodal-CoT.

Model	NAT	SOC	LAN	TXT	IMG	NO	G1-6	G7-12	Avg
Mutimodal-CoT	87.52	77.17	85.82	87.88	82.90	86.83	84.65	85.37	84.91
w/o Two-Stage Framework	80.99	87.40	81.91	80.25	78.83	83.62	82.78	82.20	82.57
w/o Vision Features	71.09	70.75	69.18	71.16	65.84	71.57	71.00	69.68	70.53

maximum input sequence length is 512. The batch sizes for the base and large models are 16 and 8, respectively. Our experiments are run on 4 NVIDIA Tesla V100 32G GPUs.

Baseline Models Following Lu et al. (2022a), our baselines include (i) Visual question answering (VQA) models (Anderson et al., 2018; Kim et al., 2018; Yu et al., 2019; Gao et al., 2019; Kim et al., 2021; Lu et al., 2021; Li et al., 2019); (ii) Text-to-text LM models. (Khashabi et al., 2020); (iii) GPT-3.5 models (Chen et al., 2020). More details are presented in Appendix B.1.

5.3. Main Results

Table 4 shows the main results. Mutimodal-CoT_{Large} outperforms GPT-3.5 by 16.51% (75.17%→91.68%) and surpasses human performance. Specifically, among the 8 question classes, Mutimodal-CoT_{Large} achieves a 21.37% (67.43%→88.80%) performance gain for the questions with paired images (IMG). Compared with existing UnifiedQA and GPT-3.5 methods that leverage image captions in the context to provide vision semantics, the results indicate that using image features is more effective. In addition, our two-stage framework contributes to the superior results according to our ablation study results in Table 5. Overall, the results verify the effectiveness of multimodality and the potential of achieving CoT reasoning with 1B-models via our two-stage framework.

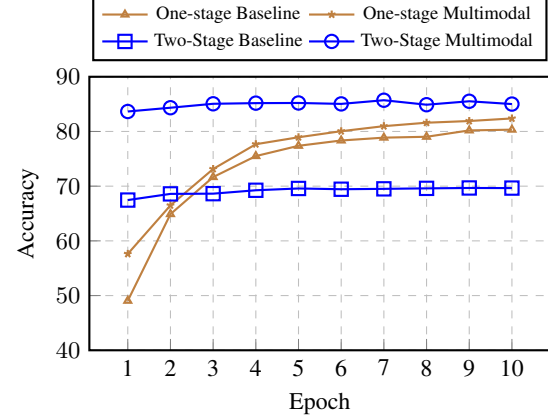


Figure 5. Accuracy curve of the No-CoT baseline and Multimodal-CoT variants across epochs.

6. Analysis

The following analysis will investigate how Multimodal-CoT works and discuss contribution factors and limitations. We use models under the base size for analysis unless otherwise stated.

6.1. Multimodality Boosts Convergence

Figure 5 shows the evaluation accuracy curve of the baseline and Multimodal-CoT in different training epochs. “One-stage” is based on the QCM→A input-output format as it

achieves the best performance in Table 2 and “Two-stage” is our two-stage framework. We find that the two-stage methods achieve relatively higher accuracy at the beginning than the one-stage baselines that generate the answer directly without CoT. It is reasonable that the two-stage methods can benefit from the generated rationales from the first training stage. However, without the vision features, the two-stage baseline could not yield better results as the training goes on due to the low-quality rationales (as observed in Section 3). In contrast, using vision features helps generate more effective rationales that contribute to better answer accuracy in our two-stage multimodal variant.

6.2. Using Different Vision Features

Different vision features may affect the model performance. We compare three widely-used types of vision features, CLIP (Radford et al., 2021), DETR (Carion et al., 2020), and ResNet (He et al., 2016). CLIP and DETR are patch-like features where DETR is based on object detection. For the ResNet features, we repeat the pooled features of ResNet-50 to the same length with the text sequence to imitate the patch-like features, where each patch is the same as the pooled image features. More details of the vision features are presented in Appendix B.2.

Table 6. Accuracy (%) of using different vision features.

Method	One-stage	Two-Stage
w/ CLIP	81.21	84.81
w/ DETR	82.57	84.91
w/ ResNet	80.97	84.77

Table 6 shows the comparative results of vision features. We observe that using vision features generally achieves better performance than the language only baseline. Specifically, DETR achieves relatively better performance in general. Therefore, we use DETR by default in Multimodal-CoT.

6.3. General Effectiveness Across Backbone Models

To test the generality of the benefits of our approach to other backbone models, we alter the underlying LMs to other variants in different sizes or types. As shown in Table 7, our approach is generally effective for the widely-used backbone models.

Table 7. Accuracy (%) with different backbone language models.

Method	Size	Language Only	Mutimodal-CoT
UnifiedQA _{Base}	223M	80.40	84.91
UnifiedQA _{Large}	738M	83.60	91.68
FLAN-T5 _{Base}	248M	83.42	85.85
FLAN-T5 _{Large}	783M	85.19	93.02

6.4. Error Analysis

To better understand the behavior of Multimodal-CoT and facilitate future studies, we manually investigate randomly selected examples generated by our approach. Table 8 summarizes the categorization results generated by Multimodal-CoT. We randomly picked up 50 samples whose answers were correct and 50 samples whose answers were incorrect. The corresponding examples from each category are presented in Appendix C.

Table 8. Categorization analysis of Multimodal-CoT.

Answer	CoT Category	Percentage (%)
Correct	CoT is correct	90
	CoT is incorrect	10
Incorrect	Commonsense Mistake	88
	Logical Mistake	12

We find that the correct samples (i.e., whose answers are correct) contain a certain amount of incorrect chain-of-thought (10%). The results indicate that CoT may not always benefit the answer inference, and the model is robust to some extent — it can predict the correct answer by ignoring incorrect rationales. For incorrect samples (i.e., whose answers are incorrect), commonsense mistake in the CoT is the most frequent error type (88%). The model often makes commonsense mistakes when answering the questions requires commonsense knowledge, e.g., understand maps and counting numbers in the images (Figure 9), and utilizing the alphabet (Figure 10). The other type of mistake is a logical mistake (12%), with contradictions in the reasoning chains (Figure 11).

The analysis indicates that there are prospective directions for future studies. It is possible to improve Multimodal-CoT by (i) incorporating more informative vision features and improving language-vision interaction to be capable of understanding maps and counting numbers; (ii) injecting commonsense knowledge; (iii) applying a filtering mechanism, e.g., using only the effective CoT to infer the answer and get rid of irrelevant CoT.

7. Conclusion

We formally study the problem of multimodal CoT. We propose Multimodal-CoT that incorporates language and vision modalities into a two-stage framework that separates rationale generation and answer inference, so answer inference can leverage better generated rationales from multimodal information. With Multimodal-CoT, we show that our method surpasses GPT-3.5 by 16% accuracy on the ScienceQA benchmark. Our error analysis shows that it is the potential to leverage more effective vision features, inject commonsense knowledge, and apply filtering mechanisms to improve CoT reasoning in future studies.

References

Anderson, P., He, X., Buehler, C., Teney, D., Johnson, M., Gould, S., and Zhang, L. Bottom-up and top-down attention for image captioning and visual question answering. In *2018 IEEE Conference on Computer Vision and Pattern Recognition, CVPR 2018, Salt Lake City, UT, USA, June 18-22, 2018*, pp. 6077–6086. IEEE Computer Society, 2018. doi: 10.1109/CVPR.2018.00636.

Brown, T. B., Mann, B., Ryder, N., Subbiah, M., Kaplan, J., Dhariwal, P., Neelakantan, A., Shyam, P., Sastry, G., Askell, A., Agarwal, S., Herbert-Voss, A., Krueger, G., Henighan, T., Child, R., Ramesh, A., Ziegler, D. M., Wu, J., Winter, C., Hesse, C., Chen, M., Sigler, E., Litwin, M., Gray, S., Chess, B., Clark, J., Berner, C., McCandlish, S., Radford, A., Sutskever, I., and Amodei, D. Language models are few-shot learners. In Larochelle, H., Ranzato, M., Hadsell, R., Balcan, M., and Lin, H. (eds.), *Advances in Neural Information Processing Systems 33: Annual Conference on Neural Information Processing Systems 2020, NeurIPS 2020, December 6-12, 2020, virtual*, 2020.

Carion, N., Massa, F., Synnaeve, G., Usunier, N., Kirillov, A., and Zagoruyko, S. End-to-end object detection with transformers. In *Computer Vision–ECCV 2020: 16th European Conference, Glasgow, UK, August 23–28, 2020, Proceedings, Part I*, pp. 213–229, 2020.

Chen, T., Kornblith, S., Swersky, K., Norouzi, M., and Hinton, G. E. Big self-supervised models are strong semi-supervised learners. In Larochelle, H., Ranzato, M., Hadsell, R., Balcan, M., and Lin, H. (eds.), *Advances in Neural Information Processing Systems 33: Annual Conference on Neural Information Processing Systems 2020, NeurIPS 2020, December 6-12, 2020, virtual*, 2020.

Chen, W., Ma, X., Wang, X., and Cohen, W. W. Program of thoughts prompting: Disentangling computation from reasoning for numerical reasoning tasks. *ArXiv preprint*, abs/2211.12588, 2022.

Chowdhery, A., Narang, S., Devlin, J., Bosma, M., Mishra, G., Roberts, A., Barham, P., Chung, H. W., Sutton, C., Gehrmann, S., Schuh, P., Shi, K., Tsvyashchenko, S., Maynez, J., Rao, A., Barnes, P., Tay, Y., Shazeer, N., Prabhakaran, V., Reif, E., Du, N., Hutchinson, B., Pope, R., Bradbury, J., Austin, J., Isard, M., Gur-Ari, G., Yin, P., Duke, T., Levskaya, A., Ghemawat, S., Dev, S., Michalewski, H., Garcia, X., Misra, V., Robinson, K., Fedus, L., Zhou, D., Ippolito, D., Luan, D., Lim, H., Zoph, B., Spiridonov, A., Sepassi, R., Dohan, D., Agrawal, S., Omernick, M., Dai, A. M., Pillai, T. S., Pellat, M., Lewkowycz, A., Moreira, E., Child, R., Polozov, O., Lee, K., Zhou, Z., Wang, X., Saeta, B., Diaz, M., Firat, O., Catasta, M., Wei, J., Meier-Hellstern, K., Eck, D., Dean, J., Petrov, S., and Fiedel, N. Palm: Scaling language modeling with pathways. *ArXiv preprint*, abs/2204.02311, 2022.

Chung, H. W., Hou, L., Longpre, S., Zoph, B., Tay, Y., Fedus, W., Li, E., Wang, X., Dehghani, M., Brahma, S., et al. Scaling instruction-finetuned language models. *arXiv preprint arXiv:2210.11416*, 2022.

Dosovitskiy, A., Beyer, L., Kolesnikov, A., Weissenborn, D., Zhai, X., Unterthiner, T., Dehghani, M., Minderer, M., Heigold, G., Gelly, S., et al. An image is worth 16x16 words: Transformers for image recognition at scale. In *The International Conference on Learning Representations (ICLR)*, 2021.

Fu, Y., Peng, H., Sabharwal, A., Clark, P., and Khot, T. Complexity-based prompting for multi-step reasoning. *ArXiv preprint*, abs/2210.00720, 2022.

Gao, P., Jiang, Z., You, H., Lu, P., Hoi, S. C. H., Wang, X., and Li, H. Dynamic fusion with intra- and inter-modality attention flow for visual question answering. In *IEEE Conference on Computer Vision and Pattern Recognition, CVPR 2019, Long Beach, CA, USA, June 16-20, 2019*, pp. 6639–6648. Computer Vision Foundation / IEEE, 2019. doi: 10.1109/CVPR.2019.00680.

He, K., Zhang, X., Ren, S., and Sun, J. Deep residual learning for image recognition. In *2016 IEEE Conference on Computer Vision and Pattern Recognition, CVPR 2016, Las Vegas, NV, USA, June 27-30, 2016*, pp. 770–778. IEEE Computer Society, 2016. doi: 10.1109/CVPR.2016.90.

Ho, N., Schmid, L., and Yun, S.-Y. Large language models are reasoning teachers. *arXiv preprint arXiv:2212.10071*, 2022.

Ji, Z., Lee, N., Frieske, R., Yu, T., Su, D., Xu, Y., Ishii, E., Bang, Y., Madotto, A., and Fung, P. Survey of hallucination in natural language generation. *ACM Computing Surveys*, 2022.

Khashabi, D., Min, S., Khot, T., Sabharwal, A., Tafjord, O., Clark, P., and Hajishirzi, H. UNIFIEDQA: Crossing format boundaries with a single QA system. In *Findings of the Association for Computational Linguistics: EMNLP 2020*, pp. 1896–1907, Online, 2020. Association for Computational Linguistics. doi: 10.18653/v1/2020. findings-emnlp.171.

Khot, T., Trivedi, H., Finlayson, M., Fu, Y., Richardson, K., Clark, P., and Sabharwal, A. Decomposed prompting: A modular approach for solving complex tasks. *ArXiv preprint*, abs/2210.02406, 2022.

Kim, J., Jun, J., and Zhang, B. Bilinear attention networks. In Bengio, S., Wallach, H. M., Larochelle, H., Grauman, K., Cesa-Bianchi, N., and Garnett, R. (eds.), *Advances in Neural Information Processing Systems 31: Annual Conference on Neural Information Processing Systems 2018, NeurIPS 2018, December 3-8, 2018, Montréal, Canada*, pp. 1571–1581, 2018.

Kim, W., Son, B., and Kim, I. Vilt: Vision-and-language transformer without convolution or region supervision. In *Proceedings of the 38th International Conference on Machine Learning (ICML)*, pp. 5583–5594, 2021.

Kojima, T., Gu, S. S., Reid, M., Matsuo, Y., and Iwasawa, Y. Large language models are zero-shot reasoners. *ArXiv preprint*, abs/2205.11916, 2022.

Li, B., Lv, C., Zhou, Z., Zhou, T., Xiao, T., Ma, A., and Zhu, J. On vision features in multimodal machine translation. In *Proceedings of the 60th Annual Meeting of the Association for Computational Linguistics (Volume 1: Long Papers)*, pp. 6327–6337, 2022a.

Li, L. H., Yatskar, M., Yin, D., Hsieh, C.-J., and Chang, K.-W. Visualbert: A simple and performant baseline for vision and language. *ArXiv preprint*, abs/1908.03557, 2019.

Li, Y., Lin, Z., Zhang, S., Fu, Q., Chen, B., Lou, J.-G., and Chen, W. On the advance of making language models better reasoners. *ArXiv preprint*, abs/2206.02336, 2022b.

Lu, P., Qiu, L., Chen, J., Xia, T., Zhao, Y., Zhang, W., Yu, Z., Liang, X., and Zhu, S.-C. Iconqa: A new benchmark for abstract diagram understanding and visual language reasoning. In *The 35th Conference on Neural Information Processing Systems (NeurIPS) Track on Datasets and Benchmarks*, 2021.

Lu, P., Mishra, S., Xia, T., Qiu, L., Chang, K.-W., Zhu, S.-C., Tafjord, O., Clark, P., and Kalyan, A. Learn to explain: Multimodal reasoning via thought chains for science question answering. *ArXiv preprint*, abs/2209.09513, 2022a.

Lu, P., Qiu, L., Chang, K.-W., Wu, Y. N., Zhu, S.-C., Rajpurohit, T., Clark, P., and Kalyan, A. Dynamic prompt learning via policy gradient for semi-structured mathematical reasoning. *ArXiv preprint*, abs/2209.14610, 2022b.

Magister, L. C., Mallinson, J., Adamek, J., Malmi, E., and Severyn, A. Teaching small language models to reason. *ArXiv preprint*, abs/2212.08410, 2022.

Radford, A., Kim, J. W., Hallacy, C., Ramesh, A., Goh, G., Agarwal, S., Sastry, G., Askell, A., Mishkin, P., Clark, J., et al. Learning transferable visual models from natural language supervision. In *International Conference on Machine Learning*, pp. 8748–8763. PMLR, 2021.

Rae, J. W., Borgeaud, S., Cai, T., Millican, K., Hoffmann, J., Song, F., Aslanides, J., Henderson, S., Ring, R., Young, S., Rutherford, E., Hennigan, T., Menick, J., Cassirer, A., Powell, R., Driessche, G. v. d., Hendricks, L. A., Rauh, M., Huang, P.-S., Glaese, A., Welbl, J., Dathathri, S., Huang, S., Uesato, J., Mellor, J., Higgins, I., Creswell, A., McAleese, N., Wu, A., Elsen, E., Jayakumar, S., Buchatskaya, E., Budden, D., Sutherland, E., Simonyan, K., Paganini, M., Sifre, L., Martens, L., Li, X. L., Kun-coror, A., Nematzadeh, A., Gribovskaya, E., Donato, D., Lazaridou, A., Mensch, A., Lespiau, J.-B., Tsimpoukelli, M., Grigorev, N., Fritz, D., Sotiaux, T., Pajarskas, M., Pohlen, T., Gong, Z., Toyama, D., d’Autume, C. d. M., Li, Y., Terzi, T., Mikulik, V., Babuschkin, I., Clark, A., Casas, D. d. L., Guy, A., Jones, C., Bradbury, J., Johnson, M., Hechtman, B., Weidinger, L., Gabriel, I., Isaac, W., Lockhart, E., Osindero, S., Rimell, L., Dyer, C., Vinyals, O., Ayoub, K., Stanway, J., Bennett, L., Hassabis, D., Kavukcuoglu, K., and Irving, G. Scaling language models: Methods, analysis & insights from training gopher. *ArXiv preprint*, abs/2112.11446, 2021.

Raffel, C., Shazeer, N., Roberts, A., Lee, K., Narang, S., Matena, M., Zhou, Y., Li, W., and Liu, P. J. Exploring the limits of transfer learning with a unified text-to-text transformer. *Journal of Machine Learning Research (JMLR)*, 21:1–67, 2020.

Rubin, O., Herzig, J., and Berant, J. Learning to retrieve prompts for in-context learning. In *Proceedings of the 2022 Conference of the North American Chapter of the Association for Computational Linguistics: Human Language Technologies*, pp. 2655–2671, 2022. doi: 10.18653/v1/2022.nacl-main.191.

Thoppilan, R., De Freitas, D., Hall, J., Shazeer, N., Kulshreshtha, A., Cheng, H.-T., Jin, A., Bos, T., Baker, L., Du, Y., Li, Y., Lee, H., Zheng, H. S., Ghafouri, A., Mene-gali, M., Huang, Y., Krikun, M., Lepikhin, D., Qin, J., Chen, D., Xu, Y., Chen, Z., Roberts, A., Bosma, M., Zhao, V., Zhou, Y., Chang, C.-C., Krivokon, I., Rusch, W., Pickett, M., Srinivasan, P., Man, L., Meier-Hellstern, K., Morris, M. R., Doshi, T., Santos, R. D., Duke, T., Soraker, J., Zevenbergen, B., Prabhakaran, V., Diaz, M., Hutchinson, B., Olson, K., Molina, A., Hoffman-John, E., Lee, J., Aroyo, L., Rajakumar, R., Butryna, A., Lamm, M., Kuzmina, V., Fenton, J., Cohen, A., Bernstein, R., Kurzweil, R., Aguera-Arcas, B., Cui, C., Croak, M., Chi, E., and Le, Q. Lamda: Language models for dialog applications. *ArXiv preprint*, abs/2201.08239, 2022.

Vaswani, A., Shazeer, N., Parmar, N., Uszkoreit, J., Jones, L., Gomez, A. N., Kaiser, L., and Polosukhin, I. Attention is all you need. In Guyon, I., von Luxburg, U., Bengio, S., Wallach, H. M., Fergus, R., Vishwanathan, S. V. N., and Garnett, R. (eds.), *Advances in Neural Information*

Processing Systems 30: Annual Conference on Neural Information Processing Systems 2017, December 4-9, 2017, Long Beach, CA, USA, pp. 5998–6008, 2017.

Wang, X., Wei, J., Schuurmans, D., Le, Q., Chi, E., and Zhou, D. Self-consistency improves chain of thought reasoning in language models. *ArXiv preprint*, abs/2203.11171, 2022a.

Wang, X., Wei, J., Schuurmans, D., Le, Q., Chi, E., and Zhou, D. Rationale-augmented ensembles in language models. *ArXiv preprint*, abs/2207.00747, 2022b.

Wei, J., Tay, Y., Bommasani, R., Raffel, C., Zoph, B., Borgeaud, S., Yogatama, D., Bosma, M., Zhou, D., Metzler, D., Chi, E. H., Hashimoto, T., Vinyals, O., Liang, P., Dean, J., and Fedus, W. Emergent abilities of large language models. *Transactions on Machine Learning Research*, 2022a. Survey Certification.

Wei, J., Wang, X., Schuurmans, D., Bosma, M., Chi, E., Le, Q., and Zhou, D. Chain of thought prompting elicits reasoning in large language models. *ArXiv preprint*, abs/2201.11903, 2022b.

Wu, Z., Kong, L., Bi, W., Li, X., and Kao, B. Good for misconceived reasons: An empirical revisiting on the need for visual context in multimodal machine translation. In *Proceedings of the 59th Annual Meeting of the Association for Computational Linguistics and the 11th International Joint Conference on Natural Language Processing (Volume 1: Long Papers)*, pp. 6153–6166, Online, 2021. Association for Computational Linguistics. doi: 10.18653/v1/2021.acl-long.480.

Yu, Z., Yu, J., Cui, Y., Tao, D., and Tian, Q. Deep modular co-attention networks for visual question answering. In *IEEE Conference on Computer Vision and Pattern Recognition, CVPR 2019, Long Beach, CA, USA, June 16-20, 2019*, pp. 6281–6290. Computer Vision Foundation / IEEE, 2019. doi: 10.1109/CVPR.2019.00644.

Zhang, Z., Chen, K., Wang, R., Utiyama, M., Sumita, E., Li, Z., and Zhao, H. Neural machine translation with universal visual representation. In *8th International Conference on Learning Representations, ICLR 2020, Addis Ababa, Ethiopia, April 26-30, 2020*. OpenReview.net, 2020.

Zhang, Z., Zhang, A., Li, M., and Smola, A. Automatic chain of thought prompting in large language models. *ArXiv preprint*, abs/2210.03493, 2022.

Zhang, Z., Chen, K., Wang, R., Utiyama, M., Sumita, E., Li, Z., and Zhao, H. Universal multimodal representation for language understanding. *IEEE Transactions on Pattern Analysis and Machine Intelligence*, pp. 1–18, 2023. doi: 10.1109/TPAMI.2023.3234170.

Zhou, D., Schärli, N., Hou, L., Wei, J., Scales, N., Wang, X., Schuurmans, D., Bousquet, O., Le, Q., and Chi, E. Least-to-most prompting enables complex reasoning in large language models. *ArXiv preprint*, abs/2205.10625, 2022.

A. Extended analysis for the challenge of Multimodal-CoT

A.1. More Examples of Misleading by Hallucinated Rationales

According to our case studies (Section 3.2), we find that the baseline tends to generate hallucinated rationales. We provide further examples as shown in Figure 6.

Problem

Question: Based on the arrows, which of the following organisms is a consumer?

Context: Below is a food web from a tundra ecosystem in Nunavut, a territory in Northern Canada. A food web models how the matter eaten by organisms moves through an ecosystem. The arrows in a food web represent how matter moves between organisms in an ecosystem.

Options: (A) mushroom (B) lichen

Gold Rationale: A food web is a model ... An organism in a food web can have more than one arrow pointing from it. This shows that the organism is eaten by more than one other organism in the food web. An organism in a food web can also have more than one arrow pointing to it. This shows that the organism eats more than one other organism in the food web. Consumers eat other organisms. So, there are arrows in a food web that point from other organisms to consumers. The mushroom has arrows pointing to it from the barren-ground caribou and the grizzly bear. So, the mushroom is a consumer. The lichen does not have any arrows pointing to it. So, the lichen is a producer, not a consumer.

Answer: The answer is (A).

Vision

Baseline

Rationale: A food web is a model ... This shows that the organism is eaten by more than one other organism in the food web. An organism in a food web can also have more than one arrow pointing to it. This shows that the organism eats more than one other organism in the food web. Consumers eat producers. So, in a food web, consumers have arrows pointing to them from producers. The mushroom has an arrow pointing to it from the mushroom. The mushroom is not a consumer, so the mushroom is not a consumer. The mushroom does not have any arrows pointing to it. So, the mushroom is not a consumer. The mushroom does not have any arrows pointing to it. So, the mushroom is not a consumer. The mushroom does not have any arrows pointing to it. So, the mushroom is not a consumer. The mushroom does not have any arrows pointing to it. So, the mushroom is not a consumer.

Answer: The answer is (B).

+ Vision Features

Rationale: A food web is a model ... An organism in a food web can have more than one arrow pointing from it. This shows that the organism is eaten by more than one other organism in the food web. An organism in a food web can also have more than one arrow pointing to it. This shows that the organism eats more than one other organism in the food web. Consumers eat producers organisms. So, in are arrows a food web that point from other organisms to consumers. The mushroom has arrows pointing to it from the n-brow mushroomibou. the lichenzzly bear. So, the mushroom is a consumer. The lichen has not have any arrows pointing to it. So, the mushroom is a consumer. Lichen is not a consumer.

Answer: The answer is (B).

Problem

Question: Compare the average kinetic energies of the particles in each sample. Which sample has the higher temperature?

Context: The diagrams below show two pure samples of gas in identical closed, rigid containers. Each colored ball represents one gas particle. Both samples have the same number of particles.

Options: (A) neither; the samples have the same temperature (B) sample A (C) sample B

Gold Rationale: The temperature of a substance depends on the average kinetic energy of the particles in the substance. The higher the average kinetic energy of the particles, the higher the temperature of the substance. The kinetic energy of a particle is determined by its mass and speed. For a pure substance, the greater the mass of each particle in the substance and the higher the average speed of the particles, the higher their average kinetic energy. Each particle in sample A has more mass than each particle in sample B. The particles in sample A also have a higher average speed than the particles in sample B. So, the particles in sample A have a higher average kinetic energy than the particles in sample B. Because the particles in sample A have the higher average kinetic energy, sample A must have the higher temperature.

Answer: The answer is (B).

Vision

Sample A	Mass of each particle: 40 u	Average particle speed: 950 m/s
Sample B	Mass of each particle: 32 u	Average particle speed: 750 m/s

Baseline

Rationale: The temperature of a substance depends on the average kinetic energy of the particles in the substance. The higher the average kinetic energy of the particles, the higher the temperature of the substance. The kinetic energy of a particle is determined by its mass and speed. For a pure substance, the greater the mass of each particle in the substance and the higher the average speed of the particles, the higher their average kinetic energy. Each particle in sample B has more mass than each particle in sample A. The particles in sample B also have a higher average speed than the particles in sample A. So, the particles in sample B have a higher average kinetic energy than the particles in sample A. Because the particles in sample B have the higher average kinetic energy, sample B must have the higher temperature.

Answer: The answer is (C).

+ Vision Features

Rationale: The temperature of a substance depends on the average kinetic energy of the particles in the substance. The higher the average kinetic energy of the particles, the higher the temperature of the substance. The kinetic energy of a particle is determined by its mass and speed. For a pure substance, the greater the mass of each particle in the substance and the higher the average speed of the particles, the higher their average kinetic energy. Each particle in sample A has more mass than each particle in sample B. The particles in sample A also have a higher average speed than the particles in sample B. So, the particles in sample A have a higher average kinetic energy than the particles in sample B. Because the particles in sample A have the higher average kinetic energy, sample A must have the higher temperature.

Answer: The answer is (B).

Figure 6. Examples of the two-stage framework without vision features (baseline) and with vision features (ours) for generating rationales and predicting answers. The upper part presents the problem details, and the lower part shows the outputs of the baseline and our method.

A.2. Two-Stage Training Performance with Different Sizes of LMs.

In Section 3, we observe that incorporating vision features helps generate more effective rationales, thus leading to improved answer accuracy. Besides incorporating vision features, it is possible to scale the LM size to mitigate the issue of incorrect rationales. Figure 7 shows the answer accuracy with $\text{UnifiedQA}_{\text{Base}}$ and $\text{UnifiedQA}_{\text{Large}}$. When using a larger LM, the accuracy of the baseline (w/o vision features) is boosted. The result indicates that scaling the LM is possible to mitigate the issue of incorrect rationales. However, the performance is still much inferior to using vision features. The result further verifies the effectiveness of our Multimodal-CoT with different sizes of LMs.

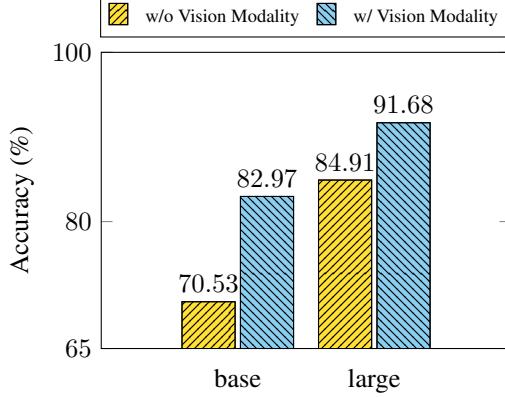


Figure 7. Answer accuracy with different sizes of LMs.

B. Experimental Details

B.1. Baseline Methods

Following Lu et al. (2022a), our baselines include three types of methods:

- (i) Visual question answering (VQA) models (Yu et al., 2019; Anderson et al., 2018; Kim et al., 2018; Gao et al., 2019; Lu et al., 2021; Li et al., 2019). The VQA baselines take the question, the context, and choices as the textual input, take the image as the vision input, and predict the score distribution over choice candidates via a linear classifier.
- (ii) Text-to-text LM models. UnifiedQA (Khashabi et al., 2020) is adopted as it is the best fine-tuning model in Lu et al. (2022a). UnifiedQA takes the textual information as the input and outputs the answer option. The image is converted into a caption extracted by an image captioning model based on ViT and GPT-2.⁶ UnifiedQA treats our task as a text generation problem. In Lu et al. (2022a), it is trained to generate a target answer text, i.e., one of the candidate options. Then, the most similar option is selected as the final prediction to evaluate the question answering accuracy.
- (iii) GPT-3.5 models (Chen et al., 2020) based on the text-davinci-002 engine. The inference is based on the few-shot prompting, where two in-context examples from the training set are concatenated before the test instance.

For UnifiedQA and GPT-3.5, CoT is applied after the answer (Lu et al., 2022a). Besides the above baselines, we develop a stronger baseline with a slight modification of the output format of UnifiedQA. Instead of predicting the answer texts, our baseline directly predicts the choice, e.g., *the answer is B*. This setting helps our baseline achieve better results than the existing UnifiedQA. Therefore, we use the stronger method as the language only baseline for analysis.

B.2. Details of Vision Features

In Section 6.2, we compared four types of vision features, CLIP (Radford et al., 2021), DETR (Carion et al., 2020), and ResNet (He et al., 2016). The specific models are: (i) CLIP: RN101;⁷ (ii) DETR: *detr_resnet101_dc5*;⁸ (iii) ResNet: we use

⁶<https://huggingface.co/nlpconnect/vit-gpt2-image-captioning>.

⁷<https://github.com/jianjieluo/OpenAI-CLIP-Feature>.

⁸<https://github.com/facebookresearch/detr>.

the averaged pooled features of a pre-trained ResNet50 CNN. Table 9 presents the dimension of the vision features (after the function `VisionExtractor(·)` in Eq. 3). For ResNet-50, we repeat the pooled features of ResNet-50 to the same length as the text sequence to imitate the patch-like features, where each patch is the same as the pooled image features.

Table 9. Dimension of vision features

Method	Dimension
CLIP	(49, 2048)
DETR	(100, 256)
ResNet	(512, 2048)

C. Examples of Case Studies

To better understand the behavior of Multimodal-CoT, we manually investigate randomly selected examples generated by our approach. Table 8 summarizes the categorization results generated by Multimodal-CoT. We randomly picked up 50 samples whose prediction results were correct and 50 samples whose prediction results were incorrect.

We find that the correct samples contain a certain amount of incorrect chain-of-thought. As shown in Figure 8(b), the model generates the incorrect rationale, “*Animals cannot their food by digesting other organisms*” but the predicted answer is correct. The result indicates that CoT may not always benefit the answer inference, and the model is robust to some extent — it can predict the correct answer by ignoring incorrect rationales.

For incorrect samples, commonsense mistake is the most frequent error type. The model also makes commonsense mistakes when answering the questions requires commonsense knowledge, e.g., understand maps and counting numbers in the images (Figure 9), and utilizing the alphabet (Figure 10). The other type of mistake is the logical mistake, where there are contradictions in the reasoning chains (Figure 11).

The analysis indicates that there are prospective directions for future studies. On the one hand, it is possible to improve the quality of CoT by (i) using more fine-grained interaction of language and vision features; and (ii) injecting commonsense knowledge. On the other hand, applying a filtering mechanism to using only the effective CoT to infer the answer and eliminate irrelevant CoT.

Problem

Question: Select the bird below.

Context: Birds have feathers, two wings, and a beak. A peregrine falcon is an example of a bird.

Options: (A) red-tailed hawk (B) tiger shark

Rationale: Birds, mammals, fish, reptiles, and amphibians are groups of animals. The animals in each group have traits in common. Scientists sort animals into groups based on traits they have in common. This process is called classification. A tiger shark is a fish. It lives underwater. It has fins, not limbs. Tiger sharks can nocturnal. They means that they are active mostly at night. A red-tailed hawk is a bird. It has feathers, two wings, and a beak. Red-tailed hawks live their be teethaks to push for pre. birds, and, rep amptiles...

Answer: The answer is (A).

----- Vision



Prediction

Rationale: Birds, mammals, fish, reptiles, and amphibians are groups of animals. The animals in each group have traits in common. Scientists sort animals into groups based on traits they have in common. This process is called classification. A tiger shark is a fish. It lives underwater. It has fins, not limbs. Tiger sharks can nocturnal. They means that they are active mostly at night. A red-tailed hawk is a bird. It has feathers, two wings, and a beak. Red-tailed hawks live their be teethaks to push for pre. birds, and, rep amptiles...

Answer: The answer is (B).

----- Vision



(a) CoT is correct

Problem

Question: Can *Leopardus wiedii* cells make their own food?

Context: This organism is *Leopardus wiedii*. It is a member of the animal kingdom. *Leopardus wiedii* is commonly called a margay. Margays live in the forest in Central and South America. Margays are nocturnal. A nocturnal animal sleeps most of the day and is awake at night.

Options: (A) no (B) yes

Rationale: In the past, scientists classified living organisms into two groups: plants and animals. Over the past 300 years, scientists have discovered many more types of organisms. Today, many scientists classify organisms into six broad groups, called kingdoms. Organisms in each kingdom have specific traits. The table below shows some traits used to describe each kingdom. | Bacteria | Archaea | Protists | Fungi | Animals | Plants. How many cells do they have? | one | one | one or many | one or many | many | many Do their cells have a nucleus? | no | no | yes | yes | yes | yes Can their cells make food? | some species can | some species can | some species can | no | no | yes *Leopardus wiedii* is an animal. Animal cells cannot make their own food. Animals get their food by digesting other organisms.

Answer: The answer is (A).

----- Vision



Prediction

Rationale: In the past, scientists classified living organisms into two groups: plants and animals. Over the past 300 years, scientists have discovered many more types of organisms. Today, many scientists classify organisms into six broad groups, called kingdoms. Organisms in each kingdom have specific traits. The table below shows some traits used to describe each kingdom. | Bacteria | Archaea | Protists | Fungi | Animals | Plants. How many cells do they have? | one | one | one or many | one or many | many | many Do their cells have a nucleus? | no | no | yes | yes | yes | yes Can their cells make food? | some species can | some species can | some species can | no | no | yes *Leopardus wiedii* is an animal. Animal cells cannot make their own food. Animals get their food by digesting other organisms.

Answer: The answer is (B).

----- Vision



(b) CoT is incorrect

Figure 8. Examples of answers are correct while the CoT is correct (a) or incorrect (b).

Problem

Question: Which ocean is highlighted?

Context: N/A

Options: (A) the Atlantic Ocean (B) the Indian Ocean
 (C) the Pacific Ocean (D) the Southern Ocean

Rationale: Oceans are huge bodies of salt water. The world has five oceans. All of the oceans are connected, making one world ocean. **This is the Pacific Ocean.**

Answer: The answer is (C).

Vision



Prediction

Rationale: Oceans are huge bodies of salt water. The world has five oceans. All of the oceans are connected, making one world ocean. **This is the Indian Ocean.**

Answer: The answer is (B).

(a) Mistakes about maps.

Problem

Question: Complete the text to describe the diagram. Solute particles moved in both directions across the permeable membrane. But more solute particles moved across the membrane (). When there was an equal concentration on both sides, the particles reached equilibrium.

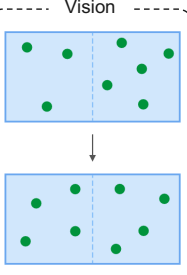
Context: The diagram below shows a solution with one solute. Each solute particle is represented by a green ball. The solution fills a closed container that is divided in half by a membrane. The membrane, represented by a dotted line, is permeable to the solute particles. The diagram shows how the solution can change over time during the process of diffusion.

Options: (A) to the left than to the right (B) to the right than to the left

Rationale: In a solution, solute particles move and spread throughout the solvent. The diagram below shows how a solution can change over time. Solute particles move from the area where they are at a higher concentration to the area where they are at a lower concentration ... Look at the diagram again. It shows you how the solution changed during the process of diffusion. Before the solute particles reached equilibrium, there were 3 solute particles on the left side of the membrane and 5 solute particles on the right side of the membrane. When the solute particles reached equilibrium, there were 4 solute particles on each side of the membrane. There was 1 more solute particle on the left side of the membrane than before. So, for the solute particles to reach equilibrium, more solute particles must have moved across the membrane to the left than to the right.

Answer: The answer is (A).

Vision



Prediction

Rationale: In a solution, solute particles move and spread throughout the solvent. The diagram below shows how a solution can change over time. Solute particles move from the area where they are at a higher concentration to the area where they are at a lower concentration ... Look at the diagram again. It shows you how the solution changed during the process of diffusion. Before the solute particles reached equilibrium, there were 5 solute particles on the left side of the membrane and 4 solute particles on the right side of the membrane. When the solute particles reached equilibrium, there were 5 solute particles on each side of the membrane. There was 1 more solute particle on the right side of the membrane than before. So, for the solute particles to reach equilibrium, more solute particles must have moved across the membrane to the right than to the left.

Answer: The answer is (B).

(b) Mistakes about counting numbers in the image.

Figure 9. Examples of commonsense mistakes about understanding maps and counting numbers.

Problem

Question: Which word would you find on a dictionary page with the following guide words? helping - hunter
Context: The diagram below shows a solution with one solute. Each solute particle is represented by a green ball. The solution fills a closed container that is divided in half by a membrane. The membrane, represented by a dotted line, is permeable to the solute particles. The diagram shows how the solution can change over time during the process of diffusion.

Options: (A) hospital (B) hardship

Rationale: Guide words appear on each page of a dictionary. They tell you the first word and last word on the page. The other words on the page come between the guide words in alphabetical order. To put words in alphabetical order, put them in order by their first letters. If the first letters are the same, look at the second letters. If the second letters are the same, look at the third letters, and so on. If one word is shorter, and there are no more letters to compare, then the shorter word comes first in alphabetical order. For example, be comes before bed. Put the words in alphabetical order. Since hospital is between the guide words helping - hunter, it would be found on that page.
Answer: The answer is (A).

Vision
N/A

Prediction

Rationale: Guide words appear on each page of a dictionary. They tell you the first word and last word on the page. The other words on the page come between the guide words in alphabetical order. To put words in alphabetical order, put them in order by their first letters. If the first letters are the same, look at the second letters. If the second letters are the same, look at the third letters, and so on. If one word is shorter, and there are no more letters to compare, then the shorter word comes first in alphabetical order. For example, be comes before bed. Put the words in alphabetical order. Since hardship is between the guide words helping - hunter, it would be found on that page.
Answer: The answer is (B).

Figure 10. Examples of commonsense mistakes about utilizing alphabet.

Problem

Question: What is the temperature of the air on a hot day?

Context: Select the better estimate.

Options: (A) 36°F (B) 36°C

Rationale : Measurements are written with both a number and a unit. The unit comes after the number. The unit shows what the number means. Temperature can be written with units of degrees Fahrenheit (°F) or Celsius (°C). Use the list below to compare the two units. 212°F | Water boils | 100 °C 98.6 °F | Body temperature | 37°C 68°F | Room temperature | 20°C 32°F | Water freezes | 0°C. The better estimate for the temperature of the air on a hot day is 36°C. 36°F is too cold.

Answer: The answer is (B).

--- Vision ---
 N/A

Prediction

Rationale: Measurements are written with both a number and a unit. The unit comes after the number. The unit shows what the number means. Temperature can be written with units of degrees Fahrenheit (°F) or Celsius (°C). Use the list below to compare the two units. 212°F | Water boils | 100 °C 98.6 °F | Body temperature | 37°C 68°F | Room temperature | 20°C 32°F | Water freezes | 0°C. The better estimate for the temperature of the air on a hot day is 36°F. 36°F is too hot.

Answer: The answer is (A).

(a) Logical mistake where the model fails at comparisons.

Problem

Question: Is this a run-on sentence? Right-handedness is controlled by genetics, interestingly enough, the same genes are also responsible for the brain becoming more specialized at certain tasks.

Context: N/A

Options: (A) yes (B) no

Rationale : A sentence is a group of words that expresses a complete thought. The band I'm in has been rehearsing daily because we have a concert in two weeks. A run-on sentence is formed when two sentences are run together, joined by just a comma or by no punctuation at all. If only a comma is used, the run-on is called a comma splice ... The band I'm in has been rehearsing daily since we have a concert in two weeks. This is a run-on sentence. It is formed a comma splice formed from two sentences run together, joined by just a comma. Right-handedness is controlled by genetics, interestingly enough, the same genes are also responsible for the brain becoming more specialized at certain tasks.

Answer: The answer is (A).

--- Vision ---
 N/A

Prediction

Rationale: A sentence is a group of words that expresses a complete thought. The band I'm in has been rehearsing daily because we have a concert in two weeks. A run-on sentence is formed when two sentences are run together, joined by just a comma or by no punctuation at all. If only a comma is used, the run-on is called a comma splice ... The band I'm in has been rehearsing daily since we have a concert in two weeks. This is not a run-on sentence. It is formed a comma splice formed from two sentences run together, joined without just a comma. Right-handedness is controlled by genetics, interestingly enough, the same genes are also responsible for the brain becoming more specialized at certain tasks.

Answer: The answer is (B).

(b) Logical mistake where the there is a contradiction in the rationale.

Figure 11. Examples of logical mistakes.